

Modeling Butanol Synthesis in Xylose by *Clostridium saccharoperbutylacetonicum*

Quan Zhou,^a Huabao Zheng,^b and Wenqiao Yuan^{a*}

To examine the effect of xylose concentration on butanol synthesis by *Clostridium saccharoperbutylacetonicum*, a kinetic model of acetone-butanol-ethanol fermentation in the media with various xylose concentrations (40 g/L to 60 g/L) was developed and implemented in COPASI. Batch fermentation experiments were conducted to feed and validate the model, and the highest butanol production was achieved in 45 g/L xylose medium. Strong correlations ($R^2 > 0.91$) between model simulation and experimental results were obtained. The modeling results suggested that the reaction rates in R_6 (from acetate to acetyl-CoA), R_8 (from acetyl-CoA to acetoacetyl-CoA), R_9 (from acetoacetyl-CoA to butyryl-CoA), R_{10} (from butyryl-CoA to butanol), R_{14} (from butyrate to butyryl-CoA), and R_{20} (xylose consumption) were higher in groups with an initial xylose of 45 g/L, 50 g/L, or 55 g/L than those in groups with 40 g/L or 60 g/L xylose. In contrast, the reaction rates in R_{13} (from butyryl-CoA to butyrate) and R_{16} (from biomass to inactive cells) were lower in groups with initial xylose of 45 g/L, 50 g/L, or 55 g/L than those in groups with 40 g/L or 60 g/L xylose, which indicated that when initial xylose concentration changed, those reactions were affected, which resulted in different butanol syntheses.

Keywords: Butanol; Xylose; Kinetic modeling; Copasi; *Clostridium saccharoperbutylacetonicum*

Contact information: a: Department of Biological and Agricultural Engineering, North Carolina State University, Raleigh, NC, 27695 USA; b; School of Environmental and Resource Sciences, Zhejiang Agricultural and Forestry University, Hangzhou, Zhejiang 311300, China; *Corresponding author: wyuan2@ncsu.edu

INTRODUCTION

It has been reported that by 2035 global energy consumption will grow by 32%, and the demand for liquid fuels will increase by 18% (USEIA 2011). To meet the growing demand for energy and to minimize the negative effects of petroleum consumption on the environment, biofuels produced from lignocellulosic biomass are promising alternatives (Tantayotai *et al.* 2017). Compared with bio-ethanol, which is widely used as the top biofuel in the U.S. market, bio-butanol yields more energy per volume or mass, and it can be blended with gasoline at higher concentrations than ethanol to fuel today's unmodified internal combustion engines (Dürre 2007).

In the traditional acetone-butanol-ethanol (ABE) fermentation process, glucose is widely used as the carbon source. Nevertheless, glucose is obtained mostly from cereal grains or sugarcane, which are food or feed sources. Compared with glucose, xylose is the second most abundant sugar in lignocellulosic biomass on earth, and it can be derived easily from agricultural residues (Li *et al.* 2015). Batch cultures using xylose have been reported successful in butanol production by *Clostridium saccharoperbutylacetonicum* (Shinto *et al.* 2008; Yao *et al.* 2017); however, the influence of xylose concentration on butanol production and associated reaction kinetics has not been systematically elucidated.

Kinetic modeling is a successful scientific approach for improving the metabolic capabilities of microorganisms due to its ability to help researchers understand, predict, and evaluate effects of adding, removing, or modifying molecular components of a cell factory, and for supporting the design of the bioreactor or fermentation process (Bailey 1991;

Stephanopoulos and Vallino 1991; Almquist *et al.* 2014). Most recent studies relevant to ABE fermentation revealed the importance of some key intermediates and the effect of product inhibition as well as substrate inhibition on butanol synthesis. Two kinetic models of ABE fermentation have been developed by Shinto *et al.* (2007; 2008) to describe the dynamic behaviors of metabolites in the ABE fermentation by *C. saccharoperbutylacetonicum* N1-4 using glucose and xylose as the carbon source, respectively. Sensitivity analysis has demonstrated that slow substrate utilization is beneficial for higher butanol production. Another kinetic model has been used to investigate the effect of various sugars on butanol synthesis by *C. acetobutylicum* DSM 792 (Raganati *et al.* 2015). Modeling results show that the uptake rate of pentose sugars is lower than that of hexose sugars. These kinetic models, however, provide no insights into the effects of xylose concentration on butanol synthesis.

The objective of this study was to understand the influence of initial xylose concentration on butanol synthesis by *C. saccharoperbutylacetonicum* N1-4. A kinetic model of ABE fermentation, using xylose as the substrate, was developed and implemented in the open-source software COPASI. The model was validated by experimental data and provided insights into the metabolic pathways of xylose to butanol influenced by substrate concentration.

EXPERIMENTAL

Materials

C. saccharoperbutylacetonicum N1-4 (ATCC 27021) was obtained from American Type Culture Collection (Manassas, VA, USA). The media and procedures used for seed culture and activation were the same as in a previous study (Zhou *et al.* 2018). Tryptone-yeast extract (TY) medium used as the pre-culture and main culture media, which consisted the following ingredients per L of distilled water: 20 g xylose (for pre-culture) or 40 g to 60 g xylose (for main culture), 2 g yeast, 6 g tryptone, 2.57 g (NH₄)₂SO₄, 0.3 g MgSO₄·7H₂O, 0.5 g KH₂PO₄, and 10 mg FeSO₄·7H₂O. In all experiments, the initial pH was adjusted to 6.5 by 5 M NaOH prior to sterilization (at 121 °C for 15 min), and during fermentation pH was measured and adjusted every 12 h to be roughly 5.5.

Methods

Batch culture and analysis

Pyrex bottles (250 mL) containing 180 mL of medium and 20 mL of inoculum were used as fermenters. Batch cultures with three replicates were carried out in TY medium with varying xylose concentrations (40 g/L, 45 g/L, 50 g/L, 55 g/L, or 60 g/L) at 30 °C under anaerobic conditions. Samples were taken every 12 h to determine the concentration of xylose, acids (lactic acid, acetic acid, and butyric acid), and solvents (acetone, butanol, ethanol) using a high performance liquid chromatograph (Prominence Series HPLC with a refractive index detector, model RID-10A, Shimadzu Corporation, Kyoto, Japan) as described in a previous study (Zhou *et al.* 2018). An OD value of 1.0 was equivalent to 0.301 g of dry cell weight per L, and the average molecular weight of *C. saccharoperbutylacetonicum* was assumed to be 172 g/mol (Shinto *et al.* 2007).

Butanol production was statistically analyzed with SAS 9.1.3 (SAS Institute Inc., Cary, NC, USA). Multiple one-way analysis of variance was conducted to evaluate the effect of initial xylose concentration on product formation (acetone, butanol, ethanol, lactic acid, acetic acid, butyric acid, and biomass) by *C. saccharoperbutylacetonicum*.

The concentration of xylose was used as the independent variable, while product (butanol) concentration was the dependent variable. Tukey's adjustment was applied to the general linear model for determining the level of significance ($P < 0.05$) among various treatments.

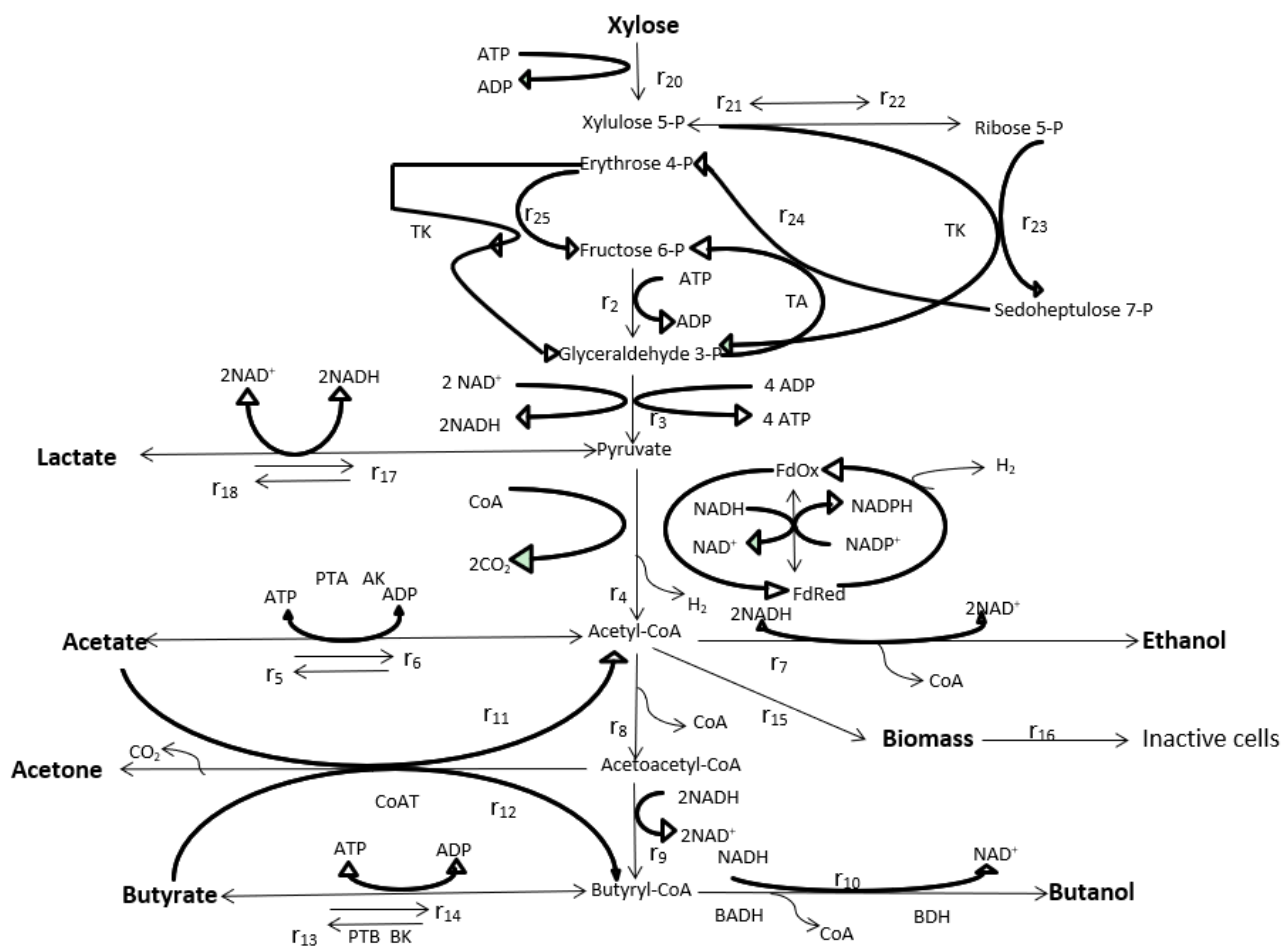


Fig. 1. The metabolic pathway of *C. acetobutylicum* using xylose as the carbon source (Raganati *et al.* 2015). Enzymes are abbreviated as follows: TA, transaldolase; TK, transketolase; PTA, phosphotransacetylase; AK, acetate kinase; CoAT, CoA transferase; PTB, phosphotransbutyrylase; BK, butyrate kinase; BADH, butyraldehyde dehydrogenase; BDH, butanol dehydrogenase

Kinetic model development

Modeling was conducted using the biochemical network simulator software COPASI (Hoops *et al.* 2006). COPASI establishes biochemical models based on the reactions between each species, and then it locates each species on a compartment that is mapped directly to the reaction network. The most attractive feature of COPASI is that it automatically converts the reactions into differential equations. The developed model, which included substrate utilization, organic acids and solvents formation, and cell growth, was established based on the ABE fermentation pathway of xylose (Fig. 1). Table 1 reports the rate equations of the metabolic reactions in the xylose utilization pathway (R_{20} to R_{25}). All the other reactions (R_2 to R_{18}) in the present model were the same as in the authors' previous study (Zhou *et al.* 2018).

Table 1. The Reaction Steps of the Kinetic Model and Associated Parameters (Raganati *et al.* 2015)

Name	Reactions	Kinetics
R ₂₀	X → X5P	$r_{20} = \frac{V_{max20}[S]}{K_{m20} + [S] + K_{m20} \left(\frac{[S]}{K_{is20}} \right)} \left(1 - \frac{[B]}{B_{max20}} \right)^{n_{B20}} F$
R ₂₁	X5P → R5P	$r_{21} = \frac{V_{max21}[X5P]}{K_{m21} + [X5P]}$
R ₂₂	R5P → X5P	$r_{22} = \frac{V_{max22}[R5P]}{K_{m22} + [R5P]}$
R ₂₃	R5P + X5P → G3P + S7P	$r_{23} = V_{max23} \left(\frac{1}{1 + K_{m23A}/[R5P]} \right) \left(\frac{1}{1 + K_{m23B}/[X5P]} \right)$
R ₂₄	G3P + S7P → E4P + F6P	$r_{24} = V_{max24} \left(\frac{1}{1 + K_{m24A}/[S7P]} \right) \left(\frac{1}{1 + K_{m24B}/[G3P]} \right)$
R ₂₅	E4P + F5P → F6P + G3P	$r_{25} = V_{max25} \left(\frac{1}{1 + K_{m25A}/[R5P]} \right) \left(\frac{1}{1 + K_{m25B}/[E4P]} \right)$

Determination of model parameters and validation

Multiple sets of kinetic parameters for the ABE fermentation under varying xylose concentrations were assessed by fitting the experimental data into the developed model. The parameters included the V_{maxj} and K_{mj} of each reaction, and the values of K_{isj} , K_{aj} , K_{msj} , K_{mjA} , K_{mjB} , B_{MAXj} , $Acet_{MAX}$, $Butyr_{MAX}$, A_{MAX} , E_{MAX} , n_{BJ} , n_{Acet} , n_{Butyr} , n_A , and n_E were estimated. The particle swarm method—an optimization algorithm of COPASI—was used for parameter estimation (Hoops *et al.* 2006). The models were validated according to the assessment of the average coefficients of determination (R^2) between the simulation results and the experimental data.

Determination of model parameters and validation

Multiple sets of kinetic parameters for the ABE fermentation under varying xylose concentrations were assessed by fitting the experimental data into the developed model. The parameters included the V_{maxj} and K_{mj} of each reaction, and the values of K_{isj} , K_{aj} , K_{msj} , K_{mjA} , K_{mjB} , B_{MAXj} , $Acet_{MAX}$, $Butyr_{MAX}$, A_{MAX} , E_{MAX} , n_{BJ} , n_{Acet} , n_{Butyr} , n_A , and n_E were estimated. The particle swarm method—an optimization algorithm of COPASI—was used for parameter estimation (Hoops *et al.* 2006). The models were validated according to the assessment of the average coefficients of determination (R^2) between the simulation results and the experimental data.

Parameter scan

A parameter scan was carried out to reveal which parameter in the pathway had a recognizable impact on butanol synthesis. By giving a 5% increase in each estimated kinetic parameter in the developed model, the percentage change in butanol could be found through parameter scan in COPASI. The impact of parameter on butanol synthesis was defined as recognizable when the 5% change in each parameter caused butanol concentration to change by at least 5%. Moreover, the reaction rates for the reactions that had recognizable impacts on butanol synthesis were calculated by taking the estimated parameters into the corresponding equations and then comparing them under various culture conditions.

RESULTS AND DISCUSSION

Batch Fermentations

Table 2 shows that as the initial xylose concentration increased from 40 g/L to 45 g/L in the medium, butanol endpoint concentration increased from 12.78 g/L to 13.45 g/L; however, no significant differences in butanol concentrations were observed among the groups of 45X, 50X, and 55X (X denotes the initial concentration of xylose in the medium, with g/L as its unit). Moreover, butanol concentration dropped to 12.37 g/L in the 60X group. With higher xylose concentration in the medium, a longer time was needed for *C. saccharoperbutylacetonicum* N1-4 to reach the exponential phase of butanol production.

As shown in Fig. 2, the fermentation progressed rapidly after 24 h in the groups of 40X and 45X, but the consumption rate of xylose and generation of butanol were slow in the first 48 h in the groups of 50X, 55X, and 60X. Additionally, the amount of xylose that was utilized by *C. saccharoperbutylacetonicum* N1-4 was not significantly different among all tested groups, which resulted in a higher butanol yield in the groups of 45X, 50X, and 55X than in the 40X group. When xylose concentration exceeded 55 g/L, butanol production showed no significant difference compared to the 40X group, which indicated that substrate saturation occurred when xylose reached 60 g/L.

Table 2. Statistical Analysis of Fermentation Results under Various Concentrations of Xylose

Xylose Concentration (g/L)	Butanol Concentration (g/L)	Xylose Utilization (g/L)	Butanol Yield (C-mol/C-mol)
40	12.77 ^b	37.83 ^a	0.55 ^b
45	13.45 ^a	36.94 ^a	0.59 ^a
50	13.31 ^a	37.02 ^a	0.58 ^a
55	12.91 ^a	36.23 ^a	0.58 ^a
60	12.37 ^b	36.70 ^a	0.53 ^b

Note: Mean values sharing the same superscript are not significantly different from each other.

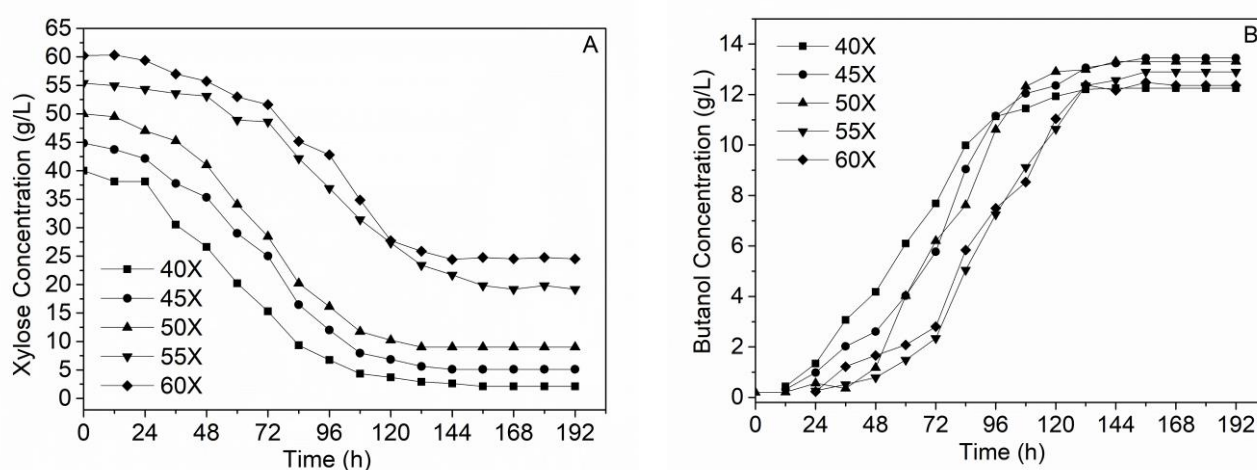


Fig. 2. The effect of xylose concentration on ABE fermentation. (A) xylose consumption profile; (B) butanol production profile. X represents g/L xylose in the medium.

Previous studies have also revealed that substrate saturation is a widespread phenomenon in enzyme kinetics that plays critical regulatory roles in many metabolic pathways

(Bisswanger 2017; Park *et al.* 2017; Kumar *et al.* 2018). To the best of the authors' knowledge, this was the first study that demonstrated the threshold level of xylose concentration (55 g/L) on butanol synthesis by *C. saccharoperbutylacetonicum* N1-4.

Comparison between Simulation Results and Experimental Time-Course Data

The estimated kinetic parameters with the initial xylose concentration of 45 g/L (299.4 mM) in the developed model are presented in Table S1 as an example. Based on the estimated parameters, the simulation results were obtained from the model and compared to the experimental results in Fig. 3.

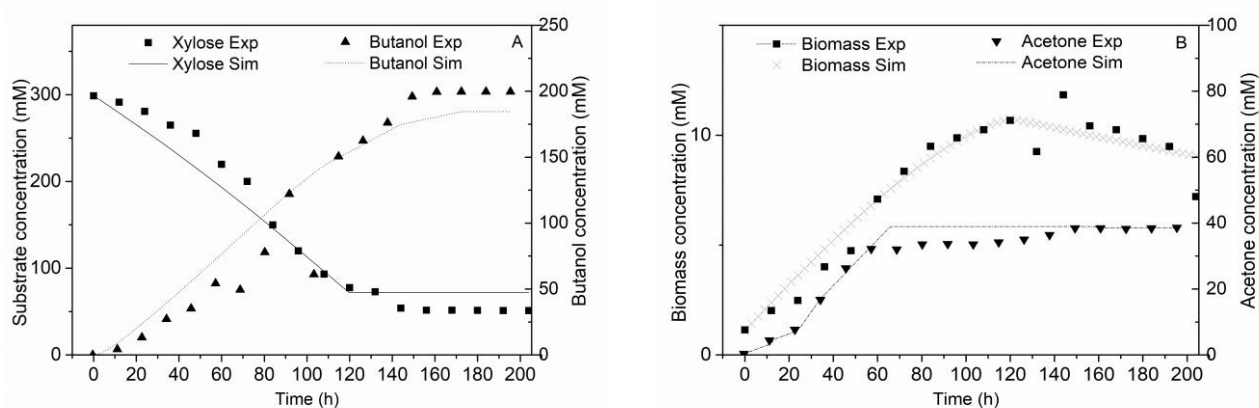


Fig. 3. The comparison between model simulation and experimental time-course data of target metabolites with 299.4 mM (45 g/L) of initial xylose concentrations: (A) time-resolved concentration of xylose and butanol; (B) time-resolved concentration of acetone and biomass

The dynamic behaviors of the important target metabolites qualitatively matched the corresponding experimental time-course data from the batch culture. The coefficient of determination (R^2) of 0.91 was obtained between the simulation results and experimental data (Table 3), which confirmed the close agreement between simulation and experimental results.

Table 3. Average Coefficients of Determination (R^2) between Simulation Results and Experimental Data

Initial Xylose Concentration (g/L)	Xylose	Acetate	Acetone	Butyrate	Butanol	Biomass
40	0.996	0.975	0.723	0.911	0.934	0.988
45	0.923	0.967	0.711	0.913	0.916	0.934
50	0.998	0.945	0.725	0.754	0.823	0.996
55	0.987	0.991	0.967	0.956	0.923	0.823
60	0.905	0.872	0.959	0.977	0.910	0.798

Parameter Scan

Kinetic models of biochemical networks elucidate how kinetic parameters affect the system/process (Hoops *et al.* 2006). In the present study, a parameter scan was used to assess the validity of the developed model and to reveal which pathway had the most significant impact on butanol synthesis. The percentage changes in predicted butanol production by giving a 5% increase in each parameter of 45X are summarized in Table 4. The reactions that had recognizable impact on endpoint butanol concentration were R_6 , R_8 , R_9 , R_{10} , R_{13} , R_{14} , R_{16} , and R_{20} . The reactions R_6 , R_8 , R_9 , R_{10} , R_{14} and R_{20} showed positive effects on butanol production. Specifically, in R_{20} , the increase in $V_{\max 20}$, K_{is20} , n_{B20} , and $B_{\max 20}$, as well as the decrease in K_{m20} ,

caused increasing endpoint butanol concentration. Calculating from Table 1, the increase in $V_{\max 20}$, K_{is20} , n_{B20} , and $B_{\max 20}$ with the decrease in K_{m20} would result in increased r_{20} , which indicated that increased r_{20} could result in increased butanol production. Therefore, R_{20} was considered to have positive effects on butanol production when xylose was utilized as the sole carbon source in the medium. Besides, as shown in Fig. 1, R_6 , R_8 , R_9 , R_{10} , and R_{14} were all involved in the pathway from acetate/butyrate to butanol. Therefore, the transition from acidogenesis phase to solventogenesis phase had favorable effects on butanol production.

R_{13} and R_{16} had negative effects on butanol production. Taking R_{13} as an example, the increase in $V_{\max 13}$ and decrease in K_{m13} caused increasing endpoint butanol concentration. Observed from Table 1, the increase in $V_{\max 13}$ and the decrease in K_{m13} would result in a lower value of r_{13} , which suggested that increasing the value of r_{13} might result in lower butanol production, which suggested that R_{13} had negative effects on butanol production.

Compared with the sensitivity analysis results in the model by Shinto *et al.* (2008), the present study revealed similar effects of R_6 , R_8 , R_9 , R_{10} , R_{13} , and R_{14} on butanol synthesis; however, the effect of xylose utilization was positive in the current study but negative in the model by Shinto *et al.* (2008). Moreover, the effects of R_{12} and R_{15} in Shinto's model were negative, but they were found not noticeable in the present study.

Table 4. Percentage Change in Endpoint Butanol Concentration in Response to a 5% Increase in Each Parameter (Only the Reactions that had Recognizable Effects are Listed)

Reaction	Parameter	Percentage change
$R_{20}^{\#}$	$V_{\max 20}$	10.66
	n_{B20}	12.37
	$B_{\max 20}$	3.11
	K_{is20}	4.03
	K_{m20}	-4.16
$R_6^{\#}$	$V_{\max 6}$	2.12
	K_{m7}	-7.13
$R_8^{\#}$	$V_{\max 8}$	4.74
	K_{m8}	-6.94
$R_9^{\#}$	$V_{\max 9}$	4.46
	K_{m9}	-7.51
$R_{10}^{\#}$	$V_{\max 10}$	10.56
	K_{m10}	-6.04
	$B_{\max 10}$	4.26
	K_{a10}	-7.21
	n_{B10}	3.86
$R_{14}^{\#}$	$V_{\max 14}$	3.56
	K_{m14}	-9.63
R_{13}^*	$V_{\max 13}$	-10.10
	K_{m13}	3.95
R_{16}^*	$V_{\max 16}$	-5.65
	K_{a16}	4.13
	K_{ms16}	-5.96

* Reactions that had negative effects on butanol production

Reactions that had positive effects on butanol production

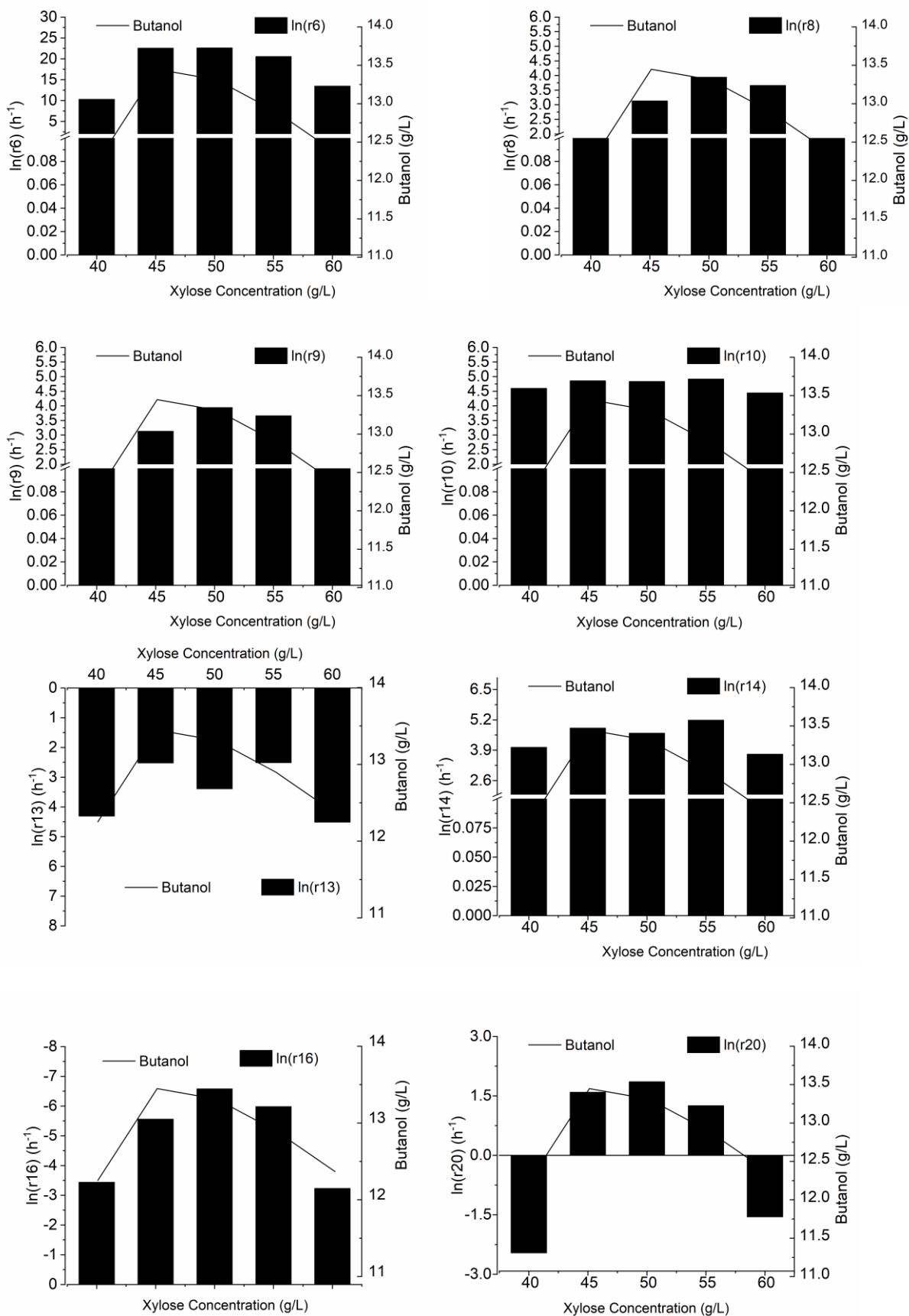


Fig. 4. The comparison between calculated reaction rates (r_6 , r_8 , r_9 , r_{10} , r_{13} , r_{14} , r_{16} , and r_{20}) and the experimental butanol concentration.

One of the possible explanations was that the formation of products from the corresponding branch metabolites in Shinto's model was all represented by single conversion, and that no regulatory effects of butyrate or butanol on butyrate re-assimilation and butanol formation were considered in Shinto's version. In the present model, a critical butanol concentration (B_{\max}) that constrained butanol-inhibited substrate uptake, cell growth, and self-inhibitory butanol generation, was introduced. Critical concentrations were also introduced for acetate, butyrate, acetone, and ethanol in the biomass equation, leading the present model to be an improved dynamic model that considered inhibitory effects of all liquid fermentation products (Millat and Winzer 2017).

To verify their effects on butanol production, the reaction rates of R_6 , R_8 , R_9 , R_{10} , R_{13} , R_{14} , R_{16} , and R_{20} were calculated by taking the estimated parameters into the corresponding equations (Table 1) under various initial xylose concentrations. Comparison between the calculated reaction rates and the experimental results of endpoint butanol concentration revealed that the changing tendency of r_6 , r_8 , r_9 , r_{10} , r_{13} , r_{14} , r_{16} , and r_{20} was qualitatively consistent with the changing trend of experimental butanol endpoint concentration under various substrate conditions.

Specifically, as shown in Fig. 4, reaction rates of R_6 , R_8 , R_9 , R_{10} , R_{14} , and R_{20} (with positive effects on butanol production) varied depending on the xylose concentration, and the preference scale to achieve higher reaction rates (r_6 , r_8 , r_9 , r_{10} , r_{14} , and r_{20}) was 45X/50X/55X > 40X/60X, which was in agreement with the experimental results. In contrast, the preference scale of xylose concentration for lower r_{13} and r_{16} (with negative effects on butanol production) was 45X/50X/55X > 40X/60X, which was also consistent with the experimental results.

The model could be used to elucidate the metabolic networks of butanol fermentation by *C. saccharoperbutylacetonicum*, and consequently to identify genetic manipulation strategies for higher bio-butanol production. When xylose is to be utilized as the sole carbon source in the medium, such strategies might include increasing the rate of xylose consumption or the conversion rates from acidogenesis phase to solventogenesis phase, or reducing the rates of biomass inactivation or conversion rate from BCoA to butyrate. For instance, xylose consumption has been successfully increased in recombinant *Saccharomyces cerevisiae* by expressing two heterologous transporters from *Arabidopsis thaliana* or by harboring the *Pichia stipitis* genes *XYL1* and *XYL2* (xylose reductase and xylitol dehydrogenase, respectively) and the endogenous *XKS1* (xylulokinase) (Jeppsson *et al.* 2003; Hector *et al.* 2008). Thus, with similar genetic engineering techniques, *C. saccharoperbutylacetonicum* might also be mutated to enhance xylose utilization rate, and butanol production could be increased consequently. In addition, some metabolic engineering strategies for ACoA and BCoA metabolism such as modulation of ACoA and BCoA generation enzymes and construction of synthetic ACoA and BCoA consuming pathways are expected to be beneficial (Zhang *et al.* 2013; Krivoruchko *et al.* 2015). Moreover, the genes that were responsible for conversion from butyrate to BCoA could be upregulated in future studies to achieve higher butanol production.

CONCLUSIONS

1. A kinetic model based on xylose metabolic pathways and COPASI was developed to simulate xylose fermentation to butanol by *C. saccharoperbutylacetonicum*. An average coefficient of determination of 0.91 was obtained between the experimental and simulation results, indicating the accuracy of the model in predicting butanol synthesis.
2. The effects of xylose concentration on butanol synthesis were elucidated by assessing the model under varying initial xylose concentrations. When xylose concentration changed, the

reaction rates of R_6 (acetate to acetyl-CoA), R_8 (acetyl-CoA to acetoacetyl-CoA), R_9 (acetoacetyl-CoA to butyryl-CoA), R_{10} (butyryl-CoA to butanol), R_{14} (butyrate to butyryl-CoA), and R_{20} (xylose consumption) also changed, which consequently resulted in different butanol syntheses.

3. This model could be used to identify genetic manipulation strategies for improving bio-butanol production by *C. saccharoperbutylacetonicum* when xylose is present in the medium as the sole carbon source. The strategies might include increasing the rate of xylose consumption or the conversion rates from acidogenesis phase to solventogenesis phase, or reducing the rates of biomass inactivation or conversion rate from BCoA to butyrate.

ACKNOWLEDGEMENTS

This work was financially supported by the USDA National Institute of Food and Agriculture, Hatch Project NC02613.

REFERENCES CITED

- Almquist, J., Cvijovic, M., Hatzimanikatis, V., Nielsen, J., and Jirstrand, M. (2014). "Kinetic models in industrial biotechnology - Improving cell factory performance," *Metab. Eng.* 24, 38-60. DOI: 10.1016/j.ymben.2014.03.007
- Bailey, J. E. (1991). "Toward a science of metabolic engineering," *Science* 252(5013), 1668-1675. DOI: 10.1126/science.2047876
- Bisswanger, H. (2017). *Enzyme Kinetics: Principles and Methods*, 3rd Edition, John Wiley & Sons, Hoboken, NJ, USA.
- Dürre, P. (2007). "Biobutanol: An attractive biofuel," *Biotechnol. J.* 2(12), 1525-1534. DOI: 10.1002/biot.200700168
- Hector, R. E., Qureshi, N., Hughes, S. R., and Cotta, M. A. (2008). "Expression of a heterologous xylose transporter in a *Saccharomyces cerevisiae* strain engineered to utilize xylose improves aerobic xylose consumption," *Appl. Microbiol. Biot.* 80(4), 675-684. DOI: 10.1007/s00253-008-1583-2
- Hoops, S., Sahle, S., Gauges, R., Lee, C., Pahle, J., Simus, N., Singhal, M., Xu, L., Mendes, P., and Kummer, U. (2006). "COPASI - A complex pathway simulator," *Bioinformatics* 22(24), 3067-3074. DOI: 10.1093/bioinformatics/btl485
- Jeppsson, M., Träff, K., Johansson, B., Hahn-Hägerdal, B., and Gorwa-Grauslund, M. F. (2003). "Effect of enhanced xylose reductase activity on xylose consumption and product distribution in xylose-fermenting recombinant *Saccharomyces cerevisiae*," *FEMS Yeast Res.* 3(2), 167-175. DOI: 10.1016/S1567-1356(02)00186-1
- Krivoruchko, A., Zhang, Y., Siewers, V., Chen, Y., and Nielsen, J. (2015). "Microbial acetyl-CoA metabolism and metabolic engineering," *Metab. Eng.* 28, 28-42. DOI: 10.1016/j.ymben.2014.11.009
- Kumar, V., Kothari, R., Pathak, V. V., and Tyagi, S. (2018). "Optimization of substrate concentration for sustainable biohydrogen production and kinetics from sugarcane molasses: Experimental and economical assessment," *Waste Biomass Valori.* 9(2), 273-281. DOI: 10.1007/s12649-016-9760-5
- Li, W., Li, M., Zheng, L., Liu, Y., Zhang, Y., Yu, Z., Ma, Z., and Li, Q. (2015). "Simultaneous utilization of glucose and xylose for lipid accumulation in black soldier fly," *Biotechnol. Biofuels* 8, 117. DOI: 10.1186/s13068-015-0306-z

- Millat, T., and Winzer, K. (2017). "Mathematical modelling of clostridial acetone-butanol-ethanol fermentation," *Appl. Microbiol. Biot.* 101(6), 2251-2271. DOI: 10.1007/s00253-017-8137-4
- Park, J.-H., Kim, D.-H., Kim, S.-H., Yoon, J.-J., and Park, H.-D. (2017). "Effect of substrate concentration on the competition between *Clostridium* and *Lactobacillus* during biohydrogen production," *Int. J. Hydrogen Energ.* DOI: 10.1016/j.ijhydene.2017.08.150
- Raganati, F., Procentese, A., Olivieri, G., Götz, P., Salatino, P., and Marzocchella, A. (2015). "Kinetic study of butanol production from various sugars by *Clostridium acetobutylicum* using a dynamic model," *Biochem. Eng. J.* 99, 156-166. DOI: 10.1016/j.bej.2015.03.001
- Shinto, H., Tashiro, Y., Kobayashi, G., Sekiguchi, T., Hanai, T., Kuriya, Y., Okamoto, M., and Sonomoto, K. (2008). "Kinetic study of substrate dependency for higher butanol production in acetone-butanol-ethanol fermentation," *Process Biochem.* 43(12), 1452-1461. DOI: 10.1016/j.procbio.2008.06.003
- Shinto, H., Tashiro, Y., Yamashita, M., Kobayashi, G., Sekiguchi, T., Hanai, T., Kuriya, Y., Okamoto, M., and Sonomoto, K. (2007). "Kinetic modeling and sensitivity analysis of acetone-butanol-ethanol production," *J. Biotechnol.* 131(1), 45-56. DOI: 10.1016/j.jbiotec.2007.05.005
- Stephanopoulos, G., and Vallino, J. J. (1991). "Network rigidity and metabolic engineering in metabolite overproduction," *Science* 252(5013), 1675-1681. DOI: 10.1126/science.1904627
- Tantayotai, P., Pornwongthong, P., Muenmuang, C., Phusantisampan, T., and Sriariyanun, M. (2017). "Effect of cellulase-producing microbial consortium on biogas production from lignocellulosic biomass," *Energy Proced.* 141, 180-183. DOI: 10.1016/j.egypro.2017.11.034
- U.S. Energy Information Administration (USEIA) (2011). *Annual Energy Outlook 2011: With Projections to 2035*, Washington, D. C. (<https://www.eia.gov/outlooks/archive/aeo11/>).
- Yao, D., Dong, S., Wang, P., Chen, T., Wang, J., Yue, Z.-B., and Wang, Y. (2017). "Robustness of *Clostridium saccharoperbutylacetonicum* for acetone-butanol-ethanol production: Effects of lignocellulosic sugars and inhibitors," *Fuel* 208, 549-557. DOI: 10.1016/j.fuel.2017.07.004
- Zhang, M., Galdieri, L., and Vancura, A. (2013). "The yeast AMPK homolog SNF1 regulates acetyl coenzyme A homeostasis and histone acetylation," *Mol. Cell. Biol.* 33(23), 4701-4717. DOI: 10.1128/MCB.00198-13
- Zhou, Q., Liu, Y., and Yuan, W. (2018). "Kinetic modeling of lactic acid and acetic acid effects on butanol fermentation by *Clostridium saccharoperbutylacetonicum*," *Fuel* 226, 181-189. DOI:10.1016/j.fuel.2018.04.019

Article submitted: March 27, 2018; Peer review completed: June 14, 2018; Revised version received: August 4, 2018; Accepted: August 6, 2018; Published: August 8, 2018.
DOI: 10.15376/biores.13.4.7270-7280